Cell, Vol. 95, 637–648, November 25, 1998, Copyright ©1998 by Cell Press

The Role of Tricorn Protease and Its Aminopeptidase-Interacting Factors in Cellular Protein Degradation

Noriko Tamura, Friedrich Lottspeich, Wolfgang Baumeister,* and Tomohiro Tamura
Max-Planck-Institut für Biochemie
D-82152 Martinsried
Germany

Summary

Tricorn protease was previously described as the core enzyme of a modular proteolytic system displaying multicatalytic activity. Here we elucidate the mode of cooperation between Tricorn and its interacting factors, and we identify two additional factors, F2 and F3, closely related aminopeptidases of 89 kDa. In conjunction with these three factors, Tricorn degrades oligopeptides in a sequential manner, yielding free amino acids. We have been able to reconstitute a proteolytic pathway comprising the proteasome, Tricorn, and its interacting factors, F1, F2, and F3, which converts proteins efficiently into amino acids. Therefore, it is quite likely that Tricorn also acts in vivo downstream of the proteasome and, in cooperation with its interacting factors, completes protein catabolic pathways.

Introduction

While cellular structures are continually rebuilt, balance must be maintained between anabolic and catabolic pathways. Ultimately, protein degradation should yield a pool of free amino acids for further use as a metabolic source. To avoid havoc, the degradation of proteins in vivo is subject to elaborate control mechanisms. A key element in controlling proteolysis is, in one guise or another, compartmentalization. Protein degradation can be confined to specialized membrane-bounded compartments such as the lysosome. Here control is exercised by vesicle sorting; once internalized, their proteinaceous cargo is degraded by a nonselective bulk process initiated by endopeptidases and finalized by aminopeptidases (Bohley and Seglen, 1992; Mason, 1996).

Another form of sequestering the proteolytic action from the crowded environment of the cell is self-compartmentalization (Larsen and Finley, 1997; Lupas et al., 1997; Baumeister et al., 1998). Several multisubunit proteases have converged toward a common barrel-shaped architecture that accommodates active sites in inner chambers, which are a few nanometers in size. Access to these proteolytic nanocompartments is restricted to unfolded proteins; hence, these proteases must be linked to a machinery capable of recognizing, binding, and unfolding target proteins that present appropriate cues. These tasks are performed by accessory complexes that invariably contain ATPase subunits rendering protein degradation energy dependent. The occurrence of self-compartmentalizing proteases in all three domains of life bears testimony of an old evolutionary principle. In prokaryotic cells lacking membrane-bounded compartments, ATP-dependent self-compartmentalizing proteases such as the proteasome, HslV, ClpP, or Lon are responsible for the bulk of the protein turnover.

Beyond facilitating the control of proteolysis, the confinement of the proteolytic activity to a nanocompartment inside these assemblies also provides the structural basis for the processive mode of action that is characteristic for these proteases: they do not release fragments after a single cleavage, but proceed to make multiple cleavages before finally discharging the degradation products (Thompson et al., 1994; Akopian et al., 1997). For the proteasome and for ClpP it has been shown that these products fall into a relatively narrow size range, 6 to 12 amino acid residues long. For most cells, peptides of this size are of little, if any, use and therefore should be degraded further. There is one notable exception: the immune system (MHC class I) has taken advantage of the existence of octa- and nonapeptides that abound amongst products (Heemels and Ploegh, 1995).

Recently, we found a novel self-compartmentalizing protease complex, unrelated to the proteasome, in the archaeon *Thermoplasma acidophilum*. We have given it the name Tricorn protease (TRI) in view of its peculiar structure (Tamura et al., 1996a). In conjunction with protein-interacting factors, TRI displays a broad array of peptidase activities. The basic, enzymatically fully active complex is a hexamer of 730 kDa with a very large internal cavity that we believe to harbor the active sites; this cavity can be accessed through the approximately 2.5 nm wide openings located on the 3-fold axis. In vivo, TRI appears to exist as an icosahedral capsid of 20 copies of the basic hexamer and a molecular mass of 14.6 MDa (Walz et al., 1997). We have suggested previously that this capsid, which has rather large void volumes in its "shell," may serve as an organizing center for the positioning of the interacting factors.

One of the interacting factors, F1, we have identified previously as a proline iminopeptidase, albeit with a broader substrate specificity (Tamura et al., 1996b). In this communication we characterize a second interacting factor, F2, an 89 kDa aminopeptidase. Surprisingly, we found a third interacting factor, F3, which is a close homolog of F2. We have elucidated the mode of cooperation between TRI and these interacting factors and were able to show that they degrade oligopeptides in a sequential manner. Furthermore, we present evidence that TRI and its interacting factors act downstream of the proteasome, allowing the cell to convert efficiently the pool of oligopeptides generated by the proteasome into free amino acids, thus closing the anabolic–catabolic cycle. We have been able to reconstitute the entire proteolytic pathway in vitro with recombinant enzymes.

*To whom correspondence may be addressed (e-mail: tamura@biochem.mpg.de).

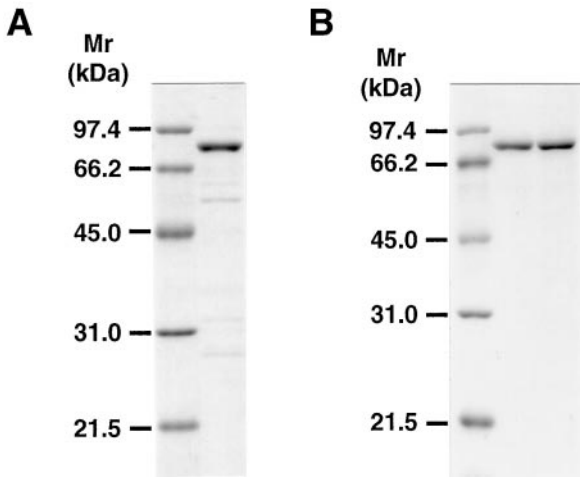

Figure 1. SDS-PAGE of Purified Tricorn Interacting Factors

(A) F2 protein isolated from *Thermoplasma acidophilum*.

(B) Recombinant F2 (left lane) and F3 (right lane) proteins.

1 μg of each protein was resolved by 12.5% of SDS-PAGE, and proteins were stained with Coomassie brilliant blue.

Results

Isolation and Cloning of Tricorn Protease Interacting Factor 2 from *Thermoplasma acidophilum*

Along with the original discovery of TRI, we found two interacting factors, termed F1 and F2, that were apparently able to modulate the activity of TRI (Tamura et al., 1996a). While F1 was identified and characterized as a proline iminopeptidase (Tamura et al., 1996b), the identity of F2 was not established at the time. In the following, we report the isolation of F2 from *Thermoplasma* cells and the cloning of its gene.

Throughout the purification procedure, the activity of F2 was monitored as an enhancement of Boc-LRR-AMC-cleaving activity upon mixing fractions with recombinant TRI. In seven chromatographic steps, 4.25 mg of F2 protein of more than 95% purity was obtained from 4.2 g of *T. acidophilum* cell crude extract. When resolved by SDS-PAGE, the isolated protein showed a single major band at 89 kDa and a few faint bands at lower molecular weight (Figure 1A). Superose12 FPLC chromatography indicated that F2 protein exists as a monomer (data not shown). The purified F2 protein was subjected to amino acid microsequencing, and six partial sequences, including the N-terminal sequence, were obtained. In order to clone the gene encoding the F2 protein, we constructed oligonucleotides and carried out linear and inverse PCR using *T. acidophilum* chromosomal DNA as a template. Sequencing of the amplified DNA revealed a 2,352 bp open reading frame (ORF) encoding 783 amino acids that contained all the peptide sequences obtained by microsequencing and had a calculated molecular weight of 88,854 kDa and an estimated pI of 5.53 (Figure 2).

A BLAST homology search displayed that the derived primary structure of F2 showed significant overall similarity to several zinc-dependent aminopeptidases from all three domains of life. The highest similarity was to an aminopeptidase from the archaeon *Sulfolobus solfataricus* (41.2% identity) (Figure 2). However, Aap1p and Ape2p from *S. cerevisiae* also showed significant similarity to F2 (Aap1p versus F2, 30.7% identity; Ape2p versus F2, 30.6% identity, respectively). The first half of the protein (residues 99–445 of F2 protein), which contains the zinc-binding motif $HExxH(x)_{18}E$ (x is any residue) at position 271–294, is highly conserved.

Unexpectedly, in the course of the ongoing *T. acidophilum* genome sequencing project in our laboratory (A. Ruepp et al., unpublished data), a gene fragment encoding 338 amino acids with high similarity to the N-terminal sequence of F2 protein was found. We cloned the gene fragment encoding the missing C-terminal region of this protein by the same experimental procedure used for cloning of the F2-encoding gene. Upon sequencing, the cloned DNA revealed a 2,343 bp ORF that encoded 780 amino acids, with a calculated molecular weight of 89,379 kDa and an estimated pI of 5.63 (Figure 2). Alignment of F2 and the newly found protein revealed an overall identity of 56.3%. Similarity was particularly high (85.5% identity) in the middle region (residues 115 to 424 of F2 protein) including the zinc-binding motif. In the following, we refer to this new protein as F3.

Expression and Characterization of the Recombinant F2 and F3 Proteins

For further characterization of F2 and F3 proteins, an expression vector was constructed that carried a $(His)_6$-tag fused to the F2 or F3 protein at the C terminus, and expressed recombinant proteins were purified by Ni-NTA affinity chromatography and hydroxyapatite chromatography (Figure 1B). As expected, both recombinant proteins showed aminopeptidase activity (Table 1). F2 protein showed a broad specificity against neutral, hydrophobic, and basic amino acid substrates with an about equal level of specific activity against H-Ala-AMC, H-Phe-AMC, H-Leu-AMC, H-Tyr-AMC, and H-Arg-AMC. F3 displayed a narrower specificity; it had a particularly strong H-Glu-AMC-hydrolyzing activity that was not observed with F1 and F2. Furthermore, both F2 and F3 released AMC from several di- and tripeptides we tested, but those activities were much lower than those found with amino acid substrates, indicating that both enzymes have a strong preference for very short peptides. Inhibitor experiments with a variety of compounds showed that the peptidase activities of both F2 and F3 were inhibited efficiently by heavy metal chelators such as *o*-phenanthroline and EDTA and also by the aminopeptidase inhibitor bestatin (data not shown).

To investigate whether F2 or F3 protein enhanced peptidase activities upon mixing them with TRI, we measured peptidase activities against several synthetic fluorogenic peptides (Table 2). F2 in conjunction with TRI indeed showed dramatically enhanced peptidase activities against several synthetic peptides (Boc-LRR-AMC, Suc-LLVY-AMC, Z-ARR-AMC, and Z-RR-AMC), even though each protein alone was hardly able to attack these substrates (Table 2). However, F3 in conjunction with TRI showed much less enhancement of peptidase activities. These data suggested to us that the peptidase activities generated by mixing F2 and F3 with TRI are

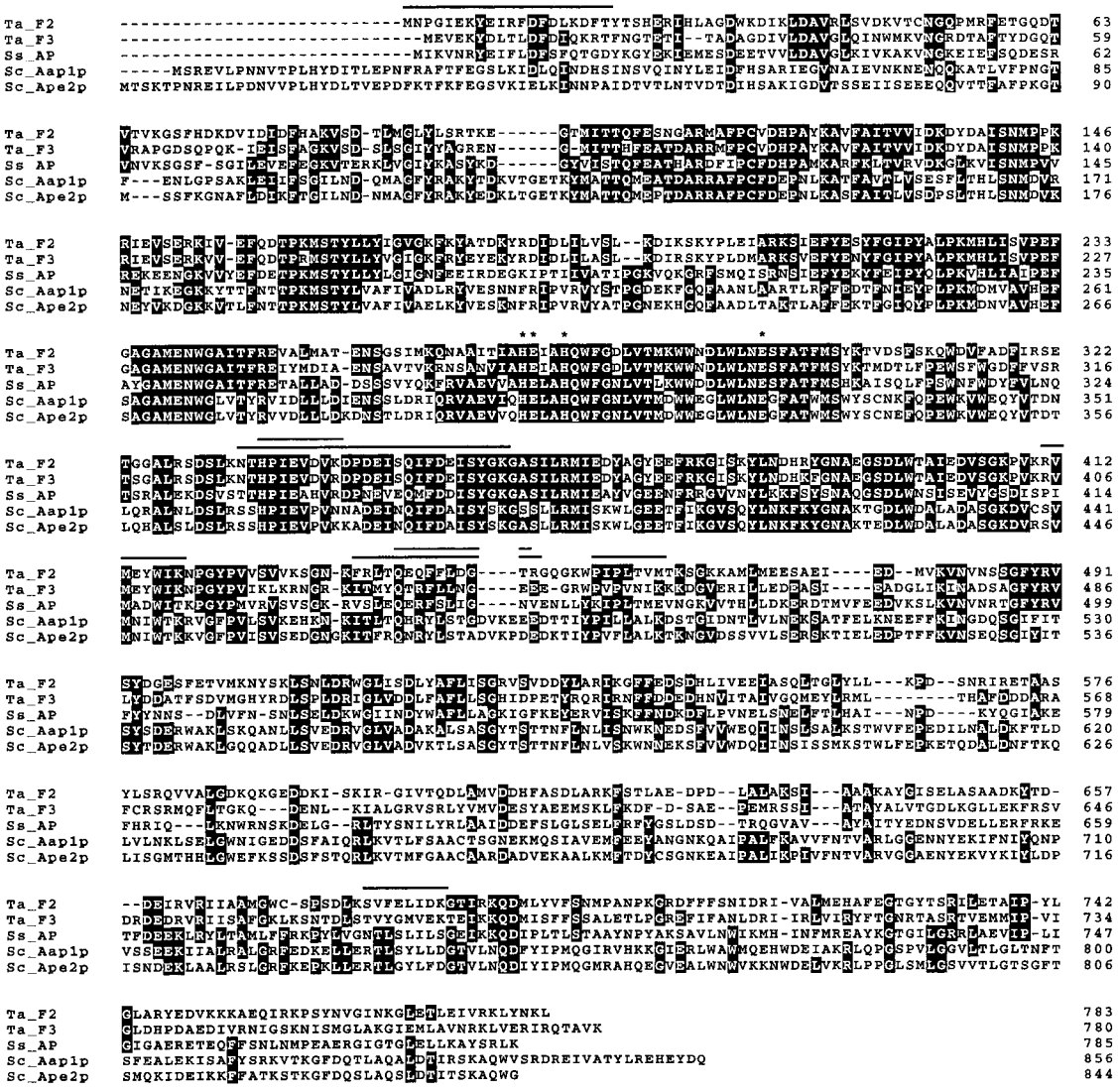

Figure 2. Sequence Alignment of F2 and F3 Proteins with Archaeal and Eukaryotic Homologs

The five aminopeptidases are from Ta, *Thermoplasma acidophilum*; Ss, *Sulfolobus solfataricus* (GenBank #Y08256); and Sc, *Saccharomyces cerevisiae* (Aap1p, GenBank #U00062; Ape2p, GenBank #Z28157). Peptide sequences that were obtained by Edman degradation are overlined, and sequences for which synthetic oligonucleotides were constructed are indicated by double overlining. Residues conserved in a majority of sequences are shown in reversed type. The consensus zinc-binding motif (HxxEH(x)18E) is marked by *. Numbers to the right refer to the amino acid position of the respective protein sequence. Alignment was performed using the PILEUP program (Genetics Computer Group).

dependent on the substrate specificities of F2 and F3 and that AMC is released from the substrates not by TRI but its interacting factors.

Tricorn Protease and Its Interacting Factor F2 Degrade Peptide Substrates Sequentially

To obtain further insights into the mode of interaction between TRI and its interacting factors, we measured peptidase activities in the presence of the protease inhibitors tosyl-L-phenylalanyl-chloromethyl ketone (TPCK) or *o*-phenanthroline (Figure 3A).

The H-AAF-AMC-cleaving activity of TRI was inactivated by TPCK in a dose-dependent manner, while F2 remained fully active; at a concentration of 100 μM TPCK, TRI lost 90% of its activity (Figure 3A, top panel). *o*-phenanthroline at 1 mM inhibited approximately 90% of the F2 H-AAF-AMC-hydrolyzing activity, while TRI retained 90% of its activity (Figure 3A, bottom panel). Interestingly, the TRI-dependent peptidase activity against Boc-LRR-AMC (see Table 2) was inactivated by both inhibitors with inhibition curves similar to those shown for F2 (with *o*-phenanthroline) or TRI (with TPCK), suggesting that both TRI and F2 activities are indeed required for efficient hydrolysis of this substrate.

In the following experiment, Boc-LRR-AMC was preincubated with either F2 or TRI, the enzymes were removed by filtration, and the flow-through fractions were incubated with the enzyme not used for preincubation (i.e., samples preincubated with TRI were now incubated with F2 and vice versa). An increase in fluorescence was

Table 1. Hydrolysis of Synthetic Substrates by Recombinant F1, F2, and F3 Proteins from *Thermoplasma acidophilum*; some of the Substrates Are Cleaved by Two or Three of Interacting Factors; Others (Boxed) Require Specific Factors for Cleavage

Substrate	F1[a]	F2	F3
Amino acids	μmol/min/mg		
H-Leu-AMC	25.8	31.0	34.7
H-Ala-AMC	55.6	26.3	15.0
H-Phe-AMC	37.1	34.4	0.8
H-Val-AMC	5.0	1.2	1.0
H-Gly-AMC	5.9	1.0	1.1
H-Pro-AMC	**37.1**	2.7	3.0
H-Tyr-AMC	4.7	**20.0**	0.7
H-Arg-AMC	0.0	**23.1**	0.6
H-Glu-AMC	0.0	0.0	**72.4**
Peptides			
Z-Arg-Arg-AMC	0.0	0.12	0.003
H-Ala-Ala-Phe-AMC	0.9	0.5	0.01
Boc-Leu-Arg-Arg-AMC	0.0	0.09	0.004
Z-Ala-Arg-Arg-AMC	0.0	0.03	0.0
Suc-Leu-Leu-Val-Tyr-AMC	0.0	0.004	0.0

[a] Data from Tamura et al. (1996b).
Activity was assayed by incubation of recombinant proteins (2–100 ng) with 100 nmol of fluorogenic substrate (AMC, 7-amino-4-methylcoumarin) in the presence of 3 μg of BSA for 15–30 min at 60°C. The fluorescence of released AMC was measured. Boc, *t*-butyloxycarbonyl; Suc, succinyl; Z, benzyloxycarbonyl.

only observed when TRI incubation was followed by F2 incubation, but not when the order was reversed (data not shown). This result suggested to us that the TRI-dependent peptidase activity results from a sequential reaction and that TRI yields an intermediate product that is hydrolyzed further by F2. To verify this hypothesis, we continuously monitored AMC release from Boc-LRR-AMC in reactions containing different amounts of F2 and a fixed amount of TRI (Figure 3B). After initiation of the reaction by enzyme addition, the period of time required to reach steady state decreased in an F2 dose-dependent manner and showed a kinetic pattern characteristic for coupled or sequential enzymatic reactions (Roberts, 1977). We tested TRI-dependent peptidase activity using several synthetic peptides; in all cases, the activity increased in an F2 dose-dependent manner and reached a plateau upon addition of 800 ng of F2 protein (Figure 3C). These results indicated to us that TRI cleaves the peptides such that the products can be hydrolyzed efficiently by F2 and AMC is released.

To identify the type of intermediate products that are generated by TRI, four synthetic peptide substrates were incubated with TRI and subjected to mass spectrometry (Figure 3D). TRI cleaved all four peptides and generated the following intermediate products: Boc-LR(↓)R-AMC, Z-R(↓)R-AMC, and Z-AR(↓)R-AMC. Suc-LLVY-AMC was cleaved by TRI between Suc-LLV and Y-AMC, but the generated Suc-LLV peptide could not be detected clearly, possibly because of further degradation. The TRI cleavage sites and peptidase activities are summarized in Table 3. These data prove that the TRI-dependent peptidase activity results from two sequential reactions: TRI cleaves peptides, yielding intermediates that are channeled to the F2 protein to be hydrolyzed further, yielding amino acids and AMC.

Table 2. F2 and F3 Proteins Generate Novel Peptidase Activities in Conjunction with Tricorn Protease

	Boc-LRR	Suc-LLVY	Z-ARR	Z-RR
	nmol AMC/hr/reaction			
TRI	0.05	0.02	0.07	0.03
F2	0.10	0.03	0.05	0.03
F2+TRI	20.37	4.26	9.72	10.04
F3	0.0	0.01	0.0	0.0
F3+TRI	0.25	0.20	0.19	0.14

Recombinant F2 and F3 (100 ng) were incubated with 20 nmol of fluorogenic (AMC) substrate for 15 min at 60°C in the presence or absence of TRI (500 ng). The fluorescence of released AMC was measured after stopping the reaction. The Suc-LLVY-AMC-cleaving activity of TRI, which had not been shown previously (Tamura et al., 1996a), was detected in this experiment.

Tricorn Protease Acts in the Protein Degradation Pathway Downstream of the Proteasome

Preliminary experiments had shown that TRI can cleave proteins and polypeptides such as casein or the oxidized insulin B-chain. However, the rate of cleavage is rather low in comparison to that of the proteasome (data not shown). When α-casein was exposed to TRI and the newly formed α-amino groups were measured using reactions with fluorescamine, the rate of release of α-amino groups was ≈20 μM/hr. Interestingly, the rate of the release of α-amino groups by TRI was dramatically enhanced (≈100 μM/hr) when TRI was added to α-casein samples that had been preincubated with *Thermoplasma* proteasomes for 2 hr (Figure 4A). This suggested to us that TRI further hydrolyzes oligopeptides generated by the proteasome. To test this hypothesis, α-casein was exposed to proteasomes, undegraded protein and proteasomes were removed by filtration, and the flow-through fractions were incubated with TRI. In fact, TRI rapidly hydrolyzed the degradation products generated by the proteasome (Figure 4B). This indicated to us that TRI's function is to shorten oligopeptides generated by the proteasome. We postulated that cytoplasmic proteins are initially cleaved by ATP-dependent proteases such as the proteasome or protease Lon, yielding oligopeptides too large to be attacked directly by aminopeptidases. TRI degrades these oligopeptides and channels the products to its interacting factors F1, F2, and F3, which then catalyze the terminal degradation step, yielding single amino acids.

To test this hypothesis, we used oxidized insulin B-chain as a substrate and monitored its degradation upon exposure to different combinations of enzymes (Figures 5A and 5C). When incubated with an equimolar mixture of F1, F2, and F3 (Fs), no degradation was observed. When incubated with TRI, the insulin B-chain was degraded, albeit slowly; after 3 hr, 63% of the substrate was still undegraded (Figure 5A). The degradation pattern we observed was quite different from that generated by the proteasome (Pro) (Figure 5C). Interestingly, as products accumulated with time, the ratio of the respective peak areas in the chromatograms did not change (except for a single peak at 16.5 min), suggesting that TRI generates the same characteristic peptides from the beginning (Figure 5B). Thus, TRI degrades insulin B-chain in a processive manner, as do the proteasome and ClpP (Thompson et al., 1994; Akopian et al., 1997).

When the insulin B-chain was exposed to TRI in combination with the three interacting factors, most of the degradation products generated by TRI were further hydrolyzed, yielding free amino acids that appeared as retarded unbound peaks (<8 min). Obviously, the peptides generated by TRI have the right size to be degraded by aminopeptidases.

As expected, the *Thermoplasma* proteasome degraded the insulin B-chain swiftly (1/2t ≅ 30 min) (Figure 5C). The relatively complex pattern of peaks remained unchanged in its characteristics with time, indicating that the proteasome does not redigest the peptides it has generated. Therefore, peptides that are typically 6–12 residues long accumulate. When the insulin B-chain was incubated with both proteasome and TRI, the peptides generated by the proteasome were degraded further and new peaks appeared. When in the absence of TRI the three interacting factors and the proteasome were used in combination, free amino acids were generated from proteasome degradation products, appearing as retarded unbound peaks (<8 min), but several peptides remained resistant to the aminopeptidases and accumulated with time. However, when the proteasome, TRI, and the three interacting factors were used in combination, most of the degradation products generated by the proteasome disappeared quickly and eluted as unbound material. Interestingly, the time course of the disappearance of intact insulin B-chain was nearly the same with the proteasome alone and in combination with TRI; although TRI alone is able to cleave the insulin B-chain, it clearly has a preference for oligopeptides.

To obtain a better estimate of the size of insulin B-chain degradation products generated either by the proteasome alone or by the proteasome in combination with TRI, products were characterized by a size-exclusion chromatography (Figure 6A). The degradation products generated by proteasome eluted as two major peaks with molecular weights around 1000 Da and 650 Da, respectively. In the presence of TRI, a new broad peak (M_r = 300–600 Da) appeared while the aforementioned peaks decreased concomitantly. When fractions from new UV peaks were subjected to MALDI-TOF mass analysis and the spectra were compared to spectra from corresponding fractions from experiments done with proteasomes alone, the appearance of numerous new peaks in the low molecular weight range (350–600) was obvious (Figure 6B). Moreover, mass spectra of the 1000 Da, 650 Da UV peak fractions and the unfractionated cleavage mixtures also showed a clear shift of mass peaks to the low molecular weight range in the presence of TRI (data not shown). These data strongly indicate that TRI degrades and shortens oligopeptides generated by the proteasome.

To further characterize degradation products generated by TRI, we searched for peptides that the proteasome was unable to degrade. We found several such peptides and used one of them, Dynorphin A (10 residues), as a model substrate. This peptide was incubated with either TRI or the proteasome, and the degradation products were analyzed by reverse-phase HPLC and mass spectrometry. While TRI degraded the Dynorphin A peptide rapidly (1/2t = 30 min), it was hardly degraded by the proteasome (Figure 7A). Mass spectrometry showed that TRI cleaved the peptide at multiple sites, preferably after basic or hydrophobic residues (Figure 7B). Upon prolonged exposure to TRI, the majority of degradation products had a size of 3–4 residues.

Discussion

Our experimental data suggest that in *Thermoplasma* cells proteins are degraded in a pathway in which the proteasome, TRI, and its three aminopeptidase-interacting factors, F1, F2, and F3, degrade proteins in a sequential manner (Figure 8). In fact, we have been able to reconstitute the entire pathway in vitro from purified recombinant proteins.

It is well established now that the proteasome, with the assistance of regulatory complexes, degrades proteins processively (Akopian et al., 1997), generating a pool of oligopeptides. Typically, the degradation products have a size of 6 to 12 residues (Wenzel et al., 1994; Niedermann et al., 1996; Kisselev et al., 1998). In eukaryotic cells, the 20S proteasome associates with a regulatory particle, the 19S cap. This complex of about 15 different subunits provides the link to the ubiquitin system that confers specificity to proteasomal protein degradation (Coux et al., 1996). A key component of this regulatory particle is an array of AAA ATPases, which probably form six-membered rings at the entrance to the 20S core complex. This ATPase ring is believed to unfold target proteins and, perhaps, assist their translocation into the proteolytic core (Lupas et al., 1993; Rubin and Finley, 1995; Baumeister et al., 1998). Proteasomes are ubiquitous in archaea and in all hitherto sequenced archaeal genomes also AAA-ATPases closely related to those found in the 19S regulatory proteins of eukaryotes have been found. There is in fact evidence that also in archaea proteasomes degrade their target proteins in an ATP-dependent manner (P. Zwickl et al., unpublished observation). In bacteria, the occurrence of genuine proteasomes appears to be restricted to actinomycetes. All those species having proteasomes also have a gene encoding an AAA-ATPase with features characteristic for proteasomal ATPases (Wolf et al., 1998; Nagy et al., submitted). Other bacteria, including *E. coli*, possess a simpler ATP-dependent proteasome-related particle referred to as HslUV (Rohrwild et al., 1996, 1997). All these complexes are able to degrade folded proteins in an energy-dependent manner; thus, they are well disposed to make the first attack on proteins targeted for degradation.

While malfunctions of the proteasome system have serious consequences and are mostly lethal in eukaryotes (Coux et al., 1996), this is not the case with *Thermoplasma* cells. In fact, in vivo inhibition studies have shown that the proteasome is dispensable under normal growth conditions, but not when cells are exposed to stress (Ruepp et al., 1998). This indicates that *Thermoplasma* has some redundancy in its proteolytic system that allows it to compensate for the inactivation of the proteasome. An obvious candidate to provide such a backup function is the ATP-dependent protease Lon, which, according to existing genome data, is found in all archaea (including *Thermoplasma*) and bacteria. While little is known about the structure of Lon, it has been shown to generate peptides 3 to 24 amino acids in length

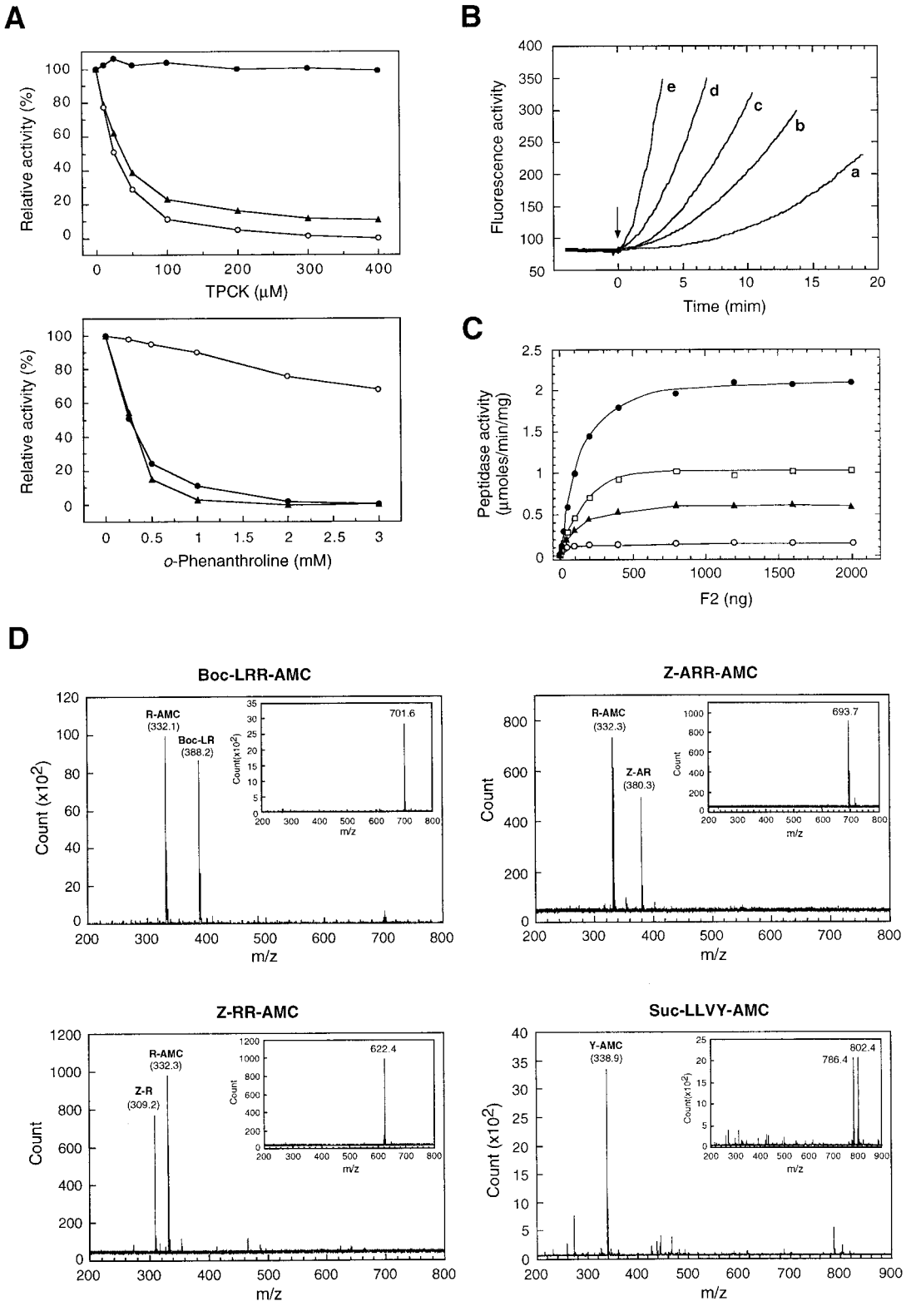

Figure 3. Tricorn Protease and Its Interacting Factor F2 Act Sequentially on Peptide Substrates

(A) Dose-dependent inhibition of TRI by TPCK (upper panel) and F2 by *o*-phenanthroline (lower panel). For inhibition by TPCK, TRI (50 ng) (open circles), F2 (1 μg) alone (closed circles), or TRI together with F2 (triangles) was incubated with TPCK in 50 μl of 50 mM Tris-HCl (pH 8.0) at 40°C for 30 min in the presence of 3 μg of BSA. Next, the reaction was initiated by the addition of 50 μl of 50 mM Tris-HCl (pH 8.0) containing 100 nmol of H-AAF-AMC and incubated at 60°C for 30 min. For inhibition by *o*-phenanthroline, F2 (200 ng) (closed circles) or TRI (1 μg) alone (open circles) or F2 together with TRI (triangles) in 100 μl of 50 mM Tris-HCl (pH 8.0) was incubated at 60°C for 15 min in the

Table 3. Tricorn Protease Cleavage Sites and Peptidase Activities

Substrate	Peptidase activity (μmol/min/mg)
↓	
Boc-LR R-AMC	2.09
↓	
Suc-LLV Y-AMC	0.15
↓	
Z-AR R-AMC	0.60
↓	
Z-R R-AMC	1.01

The substrate cleavage sites are indicated by arrows based on the measurements shown in Figure 3D. Peptides activities were calculated from the data shown in Figure 3C.

(Maurizi, 1987). In bacteria, ClpP is a common protease; its overall architecture (Wang et al., 1997) is similar to that of the 20S proteasome (Löwe et al., 1995) and HslV (Bochtler et al., 1997) and a striking example of convergent evolution. ClpP yields degradation products 7 to 10 amino acids in length (Thompson and Maurizi, 1994; Thompson et al., 1994). We conclude that there are several large proteases, some of which occur in all three domains of life, which will contribute to a cytosolic pool of oligopeptides.

Given the abundance of proteolytic systems generating such oligopeptides, it is surprising that they are a rare species (Yen et al., 1980a, 1980b); this indicates that they have very short half-lives in vivo. Our own experiments reported here and data from others (Miller, 1975) show that aminopeptidases do not degrade such oligopeptides efficiently. Thus, there is a "missing link" in the degradative pathway downstream of the proteasome, and we suggest that in *Thermoplasma* TRI provides this link. We have been able to show that the oligopeptides discharged by the proteasome are efficiently cleaved by TRI, yielding peptides that are mostly 2 to 4 residues in size. TRI appears to have a broad specificity that is advantageous for a smooth degradation of a very diverse array of oligopeptides.

Obviously the question arises as to why TRI has evolved to form such a large and elaborate structure. Since the oligopeptides generated by the proteasome are mostly of little use to the cell, it should be sufficient to scavenge them efficiently. Openings of 2.5 nm that give access to the large inner cavity of the Tricorn hexamer are sufficiently large to allow entrance of relatively large peptides; at the same time, they exclude most folded proteins from this inner compartment. This is important since, in principle, TRI is capable of degrading proteins such as casein, albeit with relatively low efficiency. The structure clearly suggests that TRI would need the assistance of an unfolding machinery to target folded proteins for degradation. The confinement of the peptidase activity to the interior of the complex also provides the structural basis for the observed processive mode of action of TRI that ensures that only short peptides and not intermediates are released. We have previously suggested that the assembly of TRI hexamers into an icosahedral capsid may provide a means to position its interacting factors and thus optimize interactions (Walz et al., 1997). Having demonstrated that TRI and its aminopeptidase-interacting factors act sequentially in degrading oligopeptides lends further support to this hypothesis. An intimate association of the interacting factors with Tricorn capsids should greatly facilitate the channeling of intermediates from one enzyme to another.

In *Thermoplasma acidophilum*, at least three different aminopeptidase-interacting factors exist. F1 is a 33 kDa proline iminopeptidase, but it in fact cleaves a wider spectrum of substrates. F1 has a number of homologs in bacteria and in eukaryotes; they are all members of the α/β hydrolase superfamily (Tamura et al., 1996b; Medrano et al., 1998). F2 (89 kDa) and F3 (89 kDa) are unrelated in sequence to F1, but they are closely related to each other (56.3% identity). All three interacting factors cleave only very short peptides (2–4 residues) efficiently. They have overlapping substrate spectra, but each of them also has specific activities: F1 is needed for the release of proline residue, F2 for the release of basic amino residues, and F3 for the release of acidic residues. Collectively, and in conjunction with TRI, they convert pools of short peptides swiftly into free amino acids.

Homologs of F2 and F3 exist in yeast. Aap1p and Ape2p from *Saccharomyces cerevisiae*, which were previously identified as metallo-aminopeptidases (Caprioglio et al., 1993; Hirsch et al., 1988), have a sequence identity of 30.7% and 30.6%, respectively, with F2. The recombinant Aap1p, expressed in *E. coli*, interacts with TRI much the same way its *Thermoplasma* homologs do (data not shown).

For TRI itself, a close homolog has so far only been found in the genome of the archaeon *Sulfolobus solfataricus* (37.1% sequence identity) (Sensen et al., 1996). From another archaeon, *Pyrococcus furiosus*, we have

presence of 3 μg BSA and 100 nmol of H-AAF-AMC. Reactions were terminated by addition of 100 μl of 10% of SDS, and released AMC was measured.

(B) Time-course plots of the concentration of AMC released in the presence of various amounts of F2 protein. In this experiment, the concentrations of substrate (200 μM) and TRI (500 ng) were fixed. For "a," 0.1 μg; "b," 0.2 μg; "c," 0.4 μg; "d," 1 μg; and "e," 2 μg of F2 protein was used. Boc-LRR-AMC were incubated at 56°C prior to addition of the enzymes TRI and F2. After reactions were initiated by addition of the enzymes (arrow), fluorescence activity was monitored by measuring the amount of released AMC.

(C) Dose dependence of F2 protein on TRI peptidase activity. TRI (50 ng) was incubated with 20 nmol of four different synthetic fluorogenic peptides, Boc-LRR-AMC (closed circles), Z-RR-AMC (squares), Z-ARR-AMC (triangles), or Suc-LLVY-AMC (open circles), in 100 μl of 50 mM Tris-HCl (pH 8.0) and the presence of different amounts of F2 protein at 60°C for 30 min. The released fluorescence (AMC) was measured.

(D) Tricorn protease generates intermediate degradation products from synthetic fluorogenic peptides. Twenty nanomoles of each substrate was incubated in 100 μl 50 mM Tris-HCl (pH 8.0) with 3 μg of TRI at 60°C for 15–60 min. The reaction was terminated by addition of 10 μl acetic acid and subjected to MALDI-TOF mass analysis. The insets show for comparison mass spectra for each substrate incubated under the same conditions as described above, but omitting TRI.

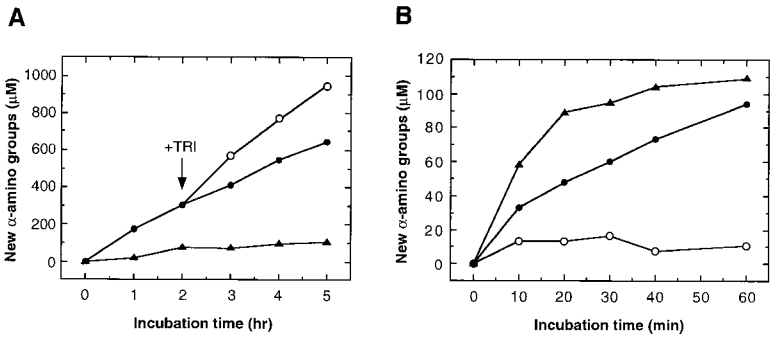

Figure 4. Oligopeptides Generated by the Proteasome Are Hydrolyzed further by Tricorn Protease

(A) Time course of casein degradation by proteasome and/or Tricorn protease. α-casein was incubated with either proteasome (closed circles) or TRI (triangles) as described under Experimental Procedures. Casein is much less efficiently hydrolyzed by TRI than by the proteasome. After a 2 hr incubation period, the reaction mixture containing the proteasome was transferred to a new tube and TRI (open circles) was added to a final concentration of 54.4 nM. The newly released α-amino groups were measured with fluorescamine.

(B) Oligopeptides generated by the proteasome are rapidly degraded by Tricorn protease. The oligopeptides generated by the proteasome were incubated with 5.4 nM (closed circles) and 13.6 nM (triangles) of TRI as described under Experimental Procedures. Control: reaction mixture without TRI (open circles). The newly released α-amino groups were measured with fluorescamine.

recently isolated a high-molecular-weight (~700 kDa) protease with similar enzymatic properties but only weak sequence similarity in the N-terminal half (T. T. et al., unpublished data). Obviously, this divergence makes it difficult to identify TRI homologs in other organisms. Glas et al. (1998) recently discovered a novel high-molecular-mass protease in the mouse lymphoma cell line EL-4; this enzyme complex appears to be capable of compensating for the loss of proteasome function. A protease with similar properties, named multicorn, was found in fission yeast (Osmulski and Gaczynska, 1998). Although the enzymatic activity and the sensitivity to the inhibitor AAF-chloromethylketone are remarkably similar to those of TRI (data not shown), there is no proof yet that those proteases are indeed related to TRI. Another candidate for a TRI-like function in higher eukaryotes is tripeptidyl peptidase II (TPPII), a subtilisin-like high-molecular-weight peptidase complex that was originally purified from cytosolic extracts of rat liver and human erythrocytes (Bålöw et al., 1986; Macpherson et al., 1987; Tomkinson and Jonsson, 1991). This enzyme releases tripeptides from the N terminus of longer peptides.

We conclude from our experiments that TRI acts as a scavenger for oligopeptides generated by the proteasome or other ATP-dependent proteases. The cleavage of these peptides into small peptides of 2 to 4 residues enables its aminopeptidase-interacting factors to hydrolyze them further, yielding free amino acids and thus completing the catabolic pathway. One would predict from this that a down-regulation or inhibition of TRI or of Tricorn-like enzymes will increase the half-lives of these oligopeptides and therefore they will accumulate in the cytosol. Since subsets of these peptides are immunocompetent, TRI and Tricorn-like molecules could become interesting therapeutic targets in cases of immunodeficiency.

Experimental Procedures

Purification of TRI Interacting Factor 2 Protein

T. acidophilum crude cell extract was prepared as described previously (Tamura et al., 1996a). Crude cell extract was loaded onto a Sephacryl S-200 column (Pharmacia) preequilibrated with buffer A (50 mM Tris-HCl [pH 7.5]). The active fractions were pooled and loaded onto a DEAE-Sephacel column (Pharmacia) also preequilibrated with buffer A. Unbound protein was collected and precipitated with ammonium sulfate at 90% saturation. The resulting pellet was dissolved in 10 ml of buffer B (50 mM potassium phosphate buffer [pH 7.0]) and loaded onto a Sephacryl S-100 column (Pharmacia) preequilibrated with the same buffer. The active fractions were pooled, ammonium sulfate added to 1.5 M, and then loaded onto a Butyl-Sepharose 4B column (Pharmacia) equilibrated with buffer B containing 1.5 M ammonium sulfate. Bound protein was eluted using a linear ammonium sulfate gradient (1.5 M–0.4 M) in buffer B. The active fractions were pooled and dialyzed against buffer C (10 mM potassium phosphate buffer [pH 7.0]) before application to a hydroxyapatite column (BioRad) preequilibrated with the same buffer. Bound proteins were eluted using a 10–300 mM phosphate linear gradient. The active fractions were pooled and dialyzed against buffer D (25 mM acetate buffer [pH 5.0]) before loading onto a CM-cellulose column (Whatman) also preequilibrated with buffer D. Bound proteins were eluted using a linear NaCl gradient (0–400 mM) in buffer D, and active fractions were pooled, dialyzed, and loaded onto a Phosphocellulose (P11) column (Whatman) preequilibrated with buffer D. Bound proteins were eluted using a linear NaCl gradient (0–600 mM) in buffer D. The active fractions were pooled, dialyzed against 50 mM Tris-HCl, 20% glycerol (pH 7.5), and stored at 4°C.

Cloning of the F2- and F3-Encoding Gene from *T. acidophilum*

Partial protein sequences of F2 were obtained by amino acid sequencing as described previously (Tamura et al., 1995). *T. acidophilum* chromosomal DNA was purified by phenol/chloroform extraction. PCR was carried out using degenerate primers that were designed based on peptide sequences HPIEVNVK (residues 336–343, N is D according to DNA sequencing) and QEQFFLDGT (residues 438–446). The primer pair was CAT CC[G/T] ATT GAG GT[G/T] AAT GT[G/T] AA and GT[G/T] CCG TC[G/T] A[A/G]G AAG AAT TGT TCT TG. The primer pair gave rise to a 332 bp fragment. The fragment was isolated, sequenced, and used to design specific primers for use in inverse PCR (Ochman et al., 1990). Inverse PCRs were continued until a full-length ORF was identified. Finally, a specific pair of primers with a XhoI site that encoded the region upstream and downstream of the F2 ORF were constructed. The amplified fragment was isolated and digested with XhoI for cloning into the same site of a pBluescript II SK(+) vector (Stratagene). Isolated plasmids were sequenced to verify their correctness.

In order to clone the gene encoding the F3 protein, the sequence data obtained from a BamHI chromosomal DNA fragment (1998 bp) that encodes the N-terminal region of the F3 protein was kindly provided by Dr. Ruepp (MPI für Biochemie, Germany). To obtain further downstream regions of this gene, primers were constructed and used for the same inverse PCR approach as used for cloning of the F2 gene, and amplified fragments were sequenced.

Construction and Expression of Recombinant F2 and F3 Proteins

F2- and F3-encoding genes were amplified by PCR using specific oligonucleotide pairs; the N-terminal primer had a flanking NdeI site, and the C-terminal primer encoded a $(His)_6$-tag with a flanking XhoI site. The amplified fragments were digested with NdeI and XhoI and

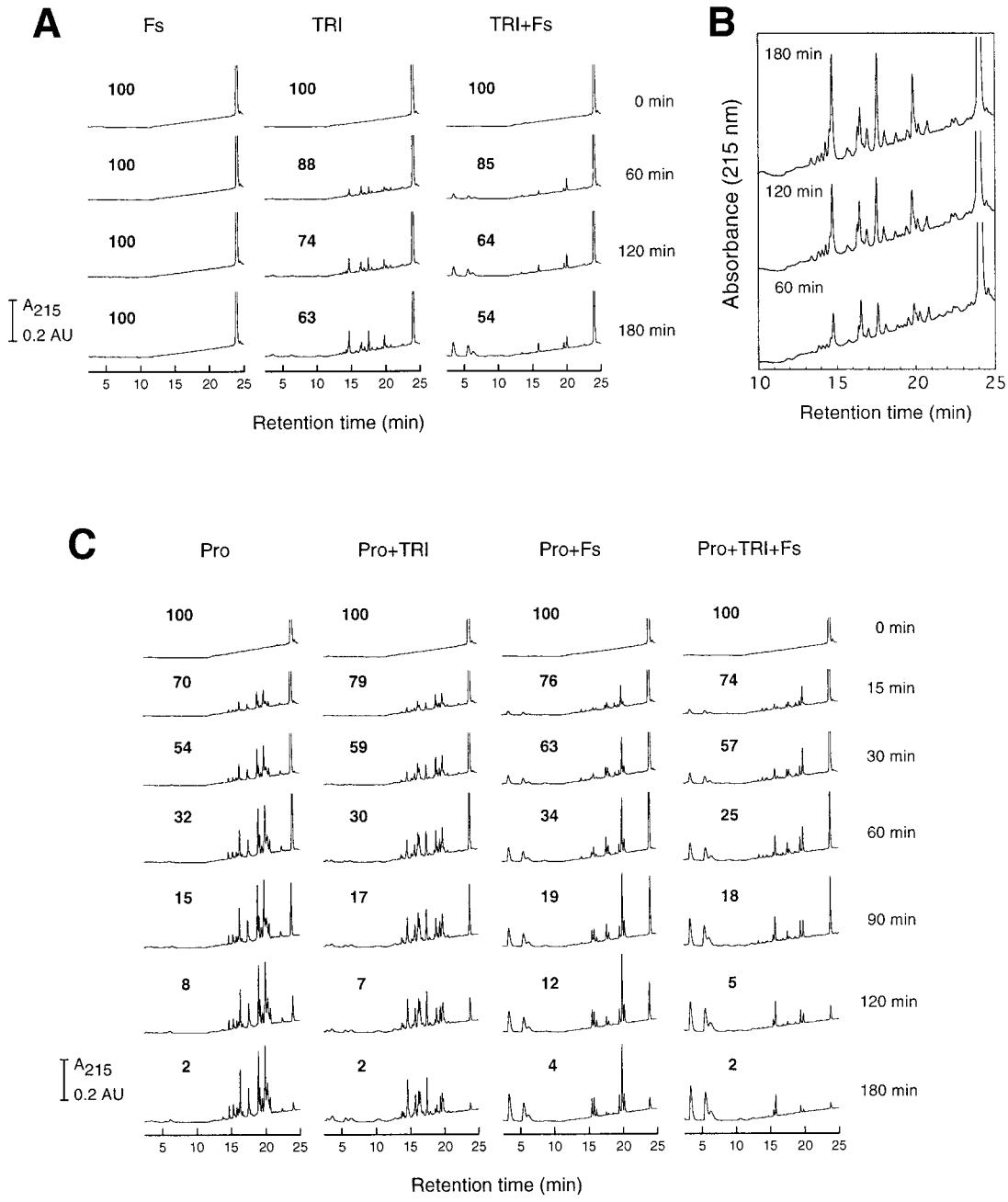

Figure 5. Reconstitution In Vitro of a Proteolytic Pathway Using Native Proteasome (Pro), Recombinant Tricorn Protease (TRI), and Its Recombinant Interacting Factors, F1, F2, and F3 (Fs)

(A and C) Insulin B-chain was exposed to proteases and degradation products were separated on a LiChroCART 125-2 Superspher RP-select B column using the buffer system described under Experimental Procedures. Each chromatogram represents the absorbance at 215 nm, and the numbers indicate the percentage of undegraded insulin B-chain. The peak area of insulin B-chain was integrated to measure the rate of disappearance. The large peak eluting at 24 min corresponds to the intact insulin B-chain.

(B) The insulin B-chain is degraded processively by Tricorn protease. Expanded views of the chromatograms of insulin B-chain degradation by TRI in (A).

cloned into the NdeI and SalI sites of a pT7-7 expression vector, yielding pT7-7-F2 and pT7-7-F3, respectively. The $(His)_6$-tagged F2 and F3 proteins were expressed in BL21 (DE3) cells containing plasmid pUBS520 (Brinkmann et al., 1989). Recombinant proteins were expressed and purified on Ni-NTA resins (Qiagen) following manufacturer instruction. Each of the active fractions containing F2 or F3 proteins were pooled and dialyzed against buffer C before application to a hydroxyapatite column preequilibrated in buffer C. Bound proteins were eluted using a linear phosphate gradient (10–300 mM), and active fractions were pooled and dialyzed against 25 mM Tris-HCl (pH 7.5) with addition of 20% glycerol before storage at −80°C.

Determination of Peptidase Activity

Throughout purification of the F2 protein, the AMC-releasing activity from Boc-LRR-AMC was monitored by addition of 1 μg recombinant TRI (Tamura et al., 1996a). For assaying activities, recombinant F2 and F3 were incubated with 10–100 nmol of substrate in 50 mM Tris-HCl (pH 8.0) at 60°C. Three micrograms of bovine serum albumin

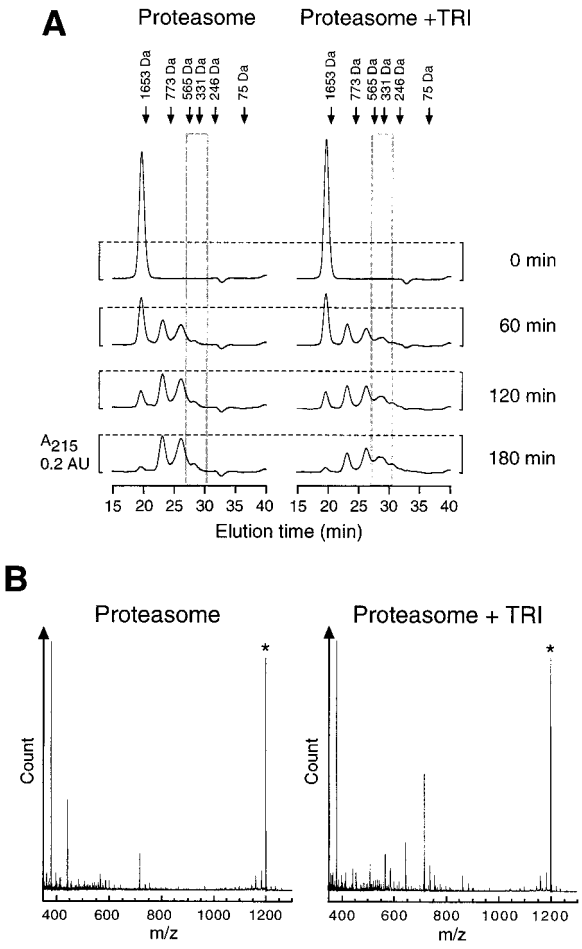

Figure 6. Size-Exclusion Chromatography of Peptides Generated from the Insulin B-Chain

(A) Elution profile of degradation products of insulin B-chain by the proteasome alone or proteasome plus Tricorn protease. Insulin B-chain was incubated with enzymes, and degradation products were separated on a Superdex Peptide PE 7.5/300 column as described under Experimental Procedures. Peptides were detected by UV absorption at 215 nm. The large peak, which elutes at 19.5 min, corresponds to the intact insulin B-chain. Peaks eluting between 300 and 600 Da are shaded in the chromatograms. The calibration markers used were ACTH (11–24, 14 amino acid residues, M_r = 1653); (Val[6], Ala[7])-kemptide (7 amino acid residues, M_r = 773); Suc-Ala-Ala-Phe-AMC (M_r = 565); H-Arg-AMC (M_r = 331); H-Ala-AMC (M_r = 246); Glycine (M_r = 75).

(B) MALDI-TOF mass analysis. Fraction eluting between 300–600 Da in (A) was collected and subjected to MALDI-TOF mass analysis. Quantification of peptides in mixtures by mass spectrometry is known to be problematic due to suppression effects (Kratzer et al., 1998). Extreme care was taken to measure the samples under standardized conditions as described under Experimental Procedures. Internal standard peptide is marked by *.

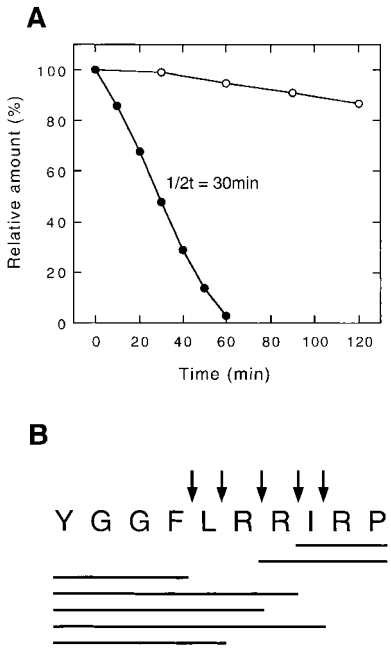

Figure 7. Tricorn Protease Generates Short Peptides from the Dynorphin A Peptide; This Peptide Is Resistant to Degradation by the Proteasome

(A) Time courses of peptide degradation by TRI and the proteasome. The Dynorphin A peptide (residues 1–10, YGGFLRRIRP, Bachem) was incubated with either TRI (closed circles) or proteasome (open circles) as described under Experimental Procedures. Degradation products were resolved by reverse-phase HPLC, and the peak area of undigested peptides was integrated to measure the rate of disappearance.

(B) Analysis of degradation products of the Dynorphin A peptide generated by TRI. The sequence is represented by single letter code and all detected cleavage sites are marked by arrows. Lines represent the peptides identified by mass spectrometry.

was added to reaction mixtures for the stabilization of F2 and F3 proteins. For terminating the reactions, 100 μl of 10% SDS and 1 ml of 0.1 M Tris-HCl (pH 9.0) were added to the 100 μl of reaction mixture. AMC released from substrates was monitored fluorometrically.

In order to measure the time course of Boc-LRR-AMC-cleaving activity, 450 μl of 50 mM Tris-HCl (pH 8.0) was preincubated with 90 nmol of substrate and 13.5 μg of bovine serum albumin at 56°C. The reaction was initiated by addition of 500 ng TRI and 0.1–2 μg of F2, and the fluorescence activity of released AMC was continuously monitored with a luminescence spectrometer LS50B (Perkin-Elmer).

Casein Degradation Assay

The amount of newly formed α-amino groups was measured using their reaction with fluorescamine (Udenfriend et al., 1972). Proteasomes were isolated from *T. acidophilum* crude cell extract as described previously (Pühler et al., 1992). α-casein (dephosphorylated, Sigma) was incubated with either the proteasome or TRI in 500 μl of 50 mM HEPES-NaOH (pH 8.0) at 60°C. The concentration of α-casein, proteasome, and TRI were 1 mg/ml, 148.6 nM, and 54.4 nM, respectively. After a 2 hr digestion of casein by the proteasome, half of the reaction solution was transferred to a new tube and, TRI was added to a final concentration of 54.4 nM.

In order to analyze the peptidase activity of TRI, α-casein was exposed to proteasomes under the same conditions as described above. After a 4 hr digestion period, proteasomes and undegraded casein were removed by filtration (Nanosep-10, Pall Gelman Sciences), and the flow-through fractions were incubated with TRI in 300 μl of 50 mM HEPES-NaOH (pH 8.0) at 60°C. The concentration of oligopeptides corresponded to 420 μM α-amino groups. TRI concentrations were 5.4 nM or 13.6 nM, respectively. Aliquots were removed at different times, and the enzymatic reaction was stopped by addition of an equal volume of 0.4% trifluoroacetic acid (TFA). Ten micrograms of the samples were mixed with 100 μl of 50 mM sodium phosphate buffer (pH 8.0) and 50 μl of an acetone solution of fluorescamine (0.3 mg/ml). The mixture was vortexed, and 1 ml of 50 mM sodium phosphate buffer (pH 8.0) was added. Fluorescence was measured fluorometrically. The amino groups generated

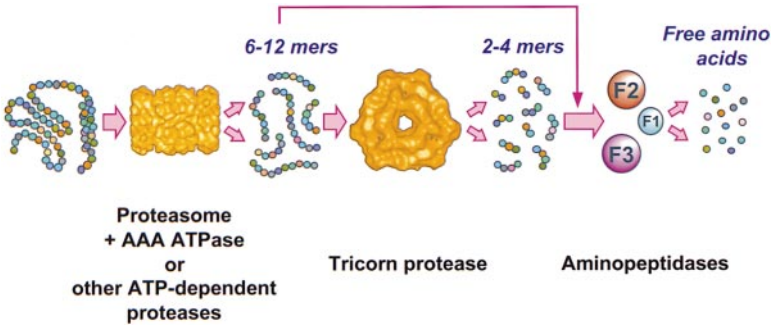

Figure 8. The Proteolytic Pathway in *Thermoplasma acidophilum*

See discussion for details.

were estimated using several concentrations of L-Leucin as a standard.

Mass Spectrometry

TRI (3 μg) was incubated with 20 nmol of fluorogenic peptides in 100 μl of 50 mM Tris-HCl (pH 8.0) at 60°C for 15–60 min. Reactions were terminated with 10 μl acetic acid. Aliquots of the solutions were analyzed by MALDI-TOF mass spectrometry.

In order to analyze the degradation products of the Dynorphin A peptide (YGGFLRRIRP, Bachem) by TRI, the peptide was incubated with TRI in 100 μl of 25 mM Tris-HCl (pH 7.5) at 60°C for 1 hr. The concentrations of peptide and TRI were 500 μM and 13.5 nM. The degradation products were resolved by reverse-phase HPLC using the same procedure as described below, and all UV peaks were analyzed by mass spectrometry. The molecular masses of peptides were calculated from the m/z peaks.

For quantitation of degradation products of insulin B-chain in Figure 6, collected UV peaks were lyophilized and redissolved with 20 μl of 10 mM Tris-HCl (pH 7.5). Internal standard solution (0.2 μl) containing either 1.66 pmol of VRKRTLRRL (monoisotopic mass = 1197.80) or 1.18 pmol of KPVGKKRRPVKVYP (monoisotopic mass = 1652.04) in 0.1% TFA/30% methanol was applied onto the target and air dried before 0.7 μl of sample was overlaid. After sample was dried, 0.7 μl of matrix solution (4-hydroxy-α-cyanocinnamic acid, 5 mg in 1 ml of 0.1% TFA/50% acetonitrile) was overlaid, dried on air, and introduced into a BRUKER Reflex III time-of-flight mass spectrometer (Bruker-Franzen, Germany). Mass analysis was performed in the positive reflector mode with delayed extraction in medium mode using a 337 nitrogen laser. The acceleration voltage, the reflector voltage, and the detector voltage were 20, 21.5, and 1.4 kV, respectively. Other parameters for measurement were as follows: deflection cut-off mass, 200; time base, 2; digitizer delay, 10,000; spectrum size, 50,000; attenuator, 98. Using exactly these conditions in each analysis, 60 shots on different regions on the target were summed up.

Reverse-Phase HPLC Analysis of Degradation Products

Recombinant proline iminopeptidase (F1) was prepared as described earlier (Tamura et al., 1996b). The oxidized insulin B-chain (Sigma) at a final concentration of 250 μM was incubated with proteases at 60°C in a reaction volume of 200 μl (50 mM Tris-HCl [pH 7.5]). The concentration of proteases were as follows: native proteasome, 74 nM; recombinant TRI, 27 nM; recombinant F1, F2, and F3 proteins, 11 nM each. At different times, aliquots of 10 μl were removed from the mixtures and 110 μl of 0.3% TFA was added to stop the reactions before storage at −20°C. One hundred microliters of a reaction mixture was analyzed by reverse-phase HPLC (ÄKTA-System; Pharmacia, equipped with a LiChroCART 125-2 Superspher RP-select B column; Merck). The column was equilibrated with 0.1% (v/v) TFA in water and eluted with a linear gradient of 0%–60% acetonitrile containing 0.08% TFA in 20 min at a flow rate of 0.3 ml/min and the gradient started 8.7 min after sample injection. Degradation products were detected by UV at 215 nm. The peak area of undigested insulin B-chain was integrated in order to measure its rate of disappearance.

The Dynorphin A peptide was incubated with either TRI or proteasome in 180 μl of 50 mM Tris-HCl (pH 7.5) at 60°C. The concentrations of peptide and enzyme used were 1 mM and 13.5 nM, respectively. The degradation rate was monitored by means of reverse-phase HPLC analysis as described above.

Size-Exclusion Chromatography of Degradation Products

All enzymes were dialyzed against 50 mM HEPES-NaOH buffer (pH 8.0). The oxidized insulin B-chain was incubated with proteases at 60°C at a final concentration of 250 μM and a total volume of 250 μl (20 mM potassium phosphate buffer [pH 7.0]). The concentration of proteases were as follows: native proteasome, 74 nM, and recombinant TRI, 27 nM. At different times, aliquots of 18 μl were removed from the mixture and 102 μl of 0.12% TFA in 35.3% acetonitrile was added to stop the reactions before storage at −20°C. One hundred microliters of reaction mixtures were analyzed by size-exclusion chromatography (ÄKTA-System, equipped with a Superdex Peptide 7.5/300; Pharmacia). Samples were resolved on the column using 0.1% (v/v) TFA in 30% acetonitrile as a running buffer at a flow rate of 0.3 ml/min. All UV peaks were collected and subjected to MALDI-TOF mass analysis as described above. The degradation products were detected by UV at 215 nm. To determine the molecular mass of eluted peptides, the column was calibrated with six peptides purchased from Bachem (see Figure 6).

Acknowledgments

We thank A. Ruepp for sharing F3 sequence data prior to publication; M. A. Kania and A. Lupas (SmithKline Beecham Pharmaceuticals) for critically reading the manuscript; M. Boicu for DNA sequencing; I. Dolenc for helpful discussions; and G. Niedermann and K. Eichmann (Max-Planck-Institute für Immunology) for drawing our attention to TPPII. This work was supported by a grant from the Human Frontier Science Program to W. B.

Received August 4, 1998; revised October 12, 1998.

References

Akopian, T.N., Kisselev, A.F., and Goldberg, A.L. (1997). Processive degradation of proteins and other catalytic properties of the proteasome from Thermoplasma acidophilum. J. Biol. Chem. *272*, 1791–1798.

Bålöw, R.-M., Tomkinson, B., Ragnarsson, U., and Zetterqvist, Ö. (1986). Purification, substrate specificity, and classification of tripeptidyl peptidase II. J. Biol. Chem. *261*, 2409–2417.

Baumeister, W., Walz, J., Zühl, F., and Seemüller, E. (1998). The proteasome: paradigm of a self-compartmentalizing protease. Cell *92*, 367–380.

Bochtler, M., Ditzel, L., Groll, M., and Huber, R. (1997). Crystal structure of heat shock locus V (HslV) from Escherichia coli. Proc. Natl. Acad. Sci. USA *94*, 6070–6074.

Bohley, P., and Seglen, P.O. (1992). Proteases and proteolysis in the lysosome. Experientia *48*, 151–157.

Brinkmann, U., Mattes, R.E., and Buckel, P. (1989). High-level expression of recombinant genes in Escherichia coli is dependent on the availability of the dnaY gene product. Gene *85*, 109–114.

Caprioglio, D.R., Padilla, C., and Werner-Washburne, M. (1993). Isolation and characterization of AAP1: a gene encoding an alanine/arginine aminopeptidase in yeast. J. Biol. Chem. *268*, 14310–14315.

Coux, O., Tanaka, K., and Goldberg, A.L. (1996). Structure and function of the 20S and 26S proteasomes. Annu. Rev. Biochem. *65*, 801–847.

Glas, R., Bogyo, M., McMaster, J.S., Gaczynska, M., and Ploegh, H.L. (1998). A proteolytic system that compensates for loss of proteasome function. Nature *392*, 618–622.

Heemels, M.-T., and Ploegh, H. (1995). Generation, translocation, and presentation of MHC class I-restricted peptides. Annu. Rev. Biochem. *64*, 463–491.

Hirsch, H.H., Rendueles, P.S., Achstetter, T., and Wolf, D.H. (1988). Aminopeptidase yscII of yeast: isolation of mutants and their biochemical and genetic analysis. Eur. J. Biochem. *173*, 589–598.

Kisselev, A.F., Akopian, T.N., and Goldberg, A.L. (1998). Range of sizes of peptide products generated during degradation of different proteins by archaeal proteasomes. J. Biol. Chem. *273*, 1982–1989.

Kratzer, R., Eckerskorn, C., Karas, M., and Lottspeich, F. (1998). Suppression effects in enzymatic peptide ladder sequencing using ultraviolet-matrix assisted laser desorption/ionization-mass spectrometry. Electrophoresis *19*, 1910–1919.

Larsen, C.N., and Finley, D. (1997). Protein translocation channels in the proteasome and other proteases. Cell *91*, 431–434.

Löwe, J., Stock, D., Jap, B., Zwickl, P., Baumeister, W., and Huber, R. (1995). Crystal structure of the 20S proteasome from the archaeon T. acidophilum at 3.4 Å resolution. Science *268*, 533–539.

Lupas, A., Koster, A.J., and Baumeister, W. (1993). Structural features of 26S and 20S proteasomes. Enzyme Protein *47*, 252–273.

Lupas, A., Flanagan, J.M., Tamura, T., and Baumeister, W. (1997). Self-compartmentalizing proteases. Trends Biochem. Sci. *22*, 399–404.

Macpherson, E., Tomkinson, B., Bålöw, R.-M., Höglund S., and Zetterqvist, Ö. (1987). Supramolecular structure of tripeptidyl peptidase II from human erythrocytes as studied by electron microscopy, and its correlation to enzyme activity. Biochem. J. *248*, 259–263.

Mason, R.W. (1996). Lysosomal metabolism of proteins. Subcell. Biochem. *27*, 159–190.

Maurizi, M.R. (1987). Degradation in vitro of bacteriophage λ N protein by Lon protease from Escherichia coli. J. Biol. Chem. *262*, 2696–2703.

Medrano, F.J., Alonso, J., García, J.L., Romero, A., Bode, W., and Gomis-Rüth, F.X. (1998). Structure of proline iminopeptidase from Xanthomonas campestris pv. citri: a prototype for the prolyl oligopeptidase family. EMBO J. *17*, 1–9.

Miller, C.G. (1975). Peptidases and proteases of Escherichia coli and Salmonella typhimurium. Annu. Rev. Microbiol. *29*, 485–504.

Niedermann, G., King, G., Butz, S., Birsner, U., Grimm, R., Shabanowitz, J., Hunt, D.F., and Eichmann, K. (1996). The proteolytic fragments generated by vertebrate proteasomes: structural relationships to major histocompatibility complex class I binding peptides. Proc. Natl. Acad. Sci. USA *93*, 8572–8577.

Ochman, H., Medhora, M.M., Garza, D., and Hartl, D.L. (1990). Amplification of flanking sequences by inverse PCR. In PCR Protocols: A Guide to Methods and Applications, M.A. Innis, D.H. Gelfand, J.J. Sninsky, and T.J. White, eds. (San Diego, California: Academic Press), pp. 219–227.

Osmulski, P.A., and Gaczynska, M. (1998). A new large proteolytic complex distinct from the proteasome is present in the cytosol of fission yeast. Curr. Biol. *8*, 1023–1026.

Pühler, G., Weinkauf, S., Bachmann, L., Müller, S., Engel, A., Hegerl, R., and Baumeister, W. (1992). Subunit stoichiometry and three-dimensional arrangement in proteasomes from Thermoplasma acidophilum. EMBO J. *4*, 1607–1616.

Roberts, D.V. (1977). Enzyme Kinetics (Cambridge: Cambridge University Press).

Rohrwild, M., Coux, O., Huang, H.-C., Moerschell, R.P., Yoo, S.J., Seol, J.H., Chung, C.H., and Goldberg, A.L. (1996). HslV-HslU: a novel ATP-dependent protease complex in Escherichia coli related to the eukaryotic proteasome. Proc. Natl. Acad. Sci. USA *93*, 5808–5813.

Rohrwild, M., Pfeifer, G., Santarius, U., Müller, S.A., Huang, H.-C., Engel, A., Baumeister, W., and Goldberg, A.L. (1997). The ATP-dependent HslVU protease from Escherichia coli is a four-ring structure resembling the proteasome. Nat. Struct. Biol. *4*, 133–139.

Rubin, D.M., and Finley, D. (1995). The proteasome: a protein-degrading organelle? Curr. Biol. *5*, 854–858.

Ruepp, A., Eckerskorn, C., Bogyo, M., and Baumeister, W. (1998). Proteasome function is dispensable under normal but not under heat shock conditions in Thermoplasma acidophilum. FEBS Lett. *425*, 87–90.

Sensen, C.W., Klenk, H.-P., Singh, R.K., Allard, G., Chan, C.C.-Y., Liu, Q.Y., Penny, S.L., Young, F., Schenk, M.E., Gaasterland, T., et al. (1996). Organizational characteristics and information content of an archaeal genome: 156 kb of sequence from Sulfolobus solfataricus P2. Mol. Microbiol. *22*, 175–191.

Tamura, T., Nagy, I., Lupas, A., Lottspeich, F., Cejka, Z., Schoofs, G., Tanaka, K., De Mot, R., and Baumeister, W. (1995). The first characterization of a eubacterial proteasome: the 20S complex of Rhodococcus. Curr. Biol. *5*, 766–774.

Tamura, T., Tamura, N., Cejka, Z., Hegerl, R., Lottspeich, F., and Baumeister, W. (1996a). Tricorn protease–the core of a modular proteolytic system. Science *274*, 1385–1389.

Tamura, T., Tamura, N., Lottspeich, F., and Baumeister, W. (1996b). Tricorn protease (TRI) interacting factor 1 from Thermoplasma acidophilum is a proline iminopeptidase. FEBS Lett. *398*, 101–105.

Thompson, M.W., and Maurizi, M.R. (1994). Activity and specificity of Escherichia coli ClpAP protease in cleaving model peptide substrates. J. Biol. Chem. *269*, 18201–18208.

Thompson, M.W., Singth, S.K., and Maurizi, M.R. (1994). Processive degradation of proteins by the ATP-dependent Clp protease from Escherichia coli. J. Biol. Chem. *269*, 18209–18215.

Tomkinson, B., and Jonsson, A.-K. (1991). Characterization of cDNA for human tripeptidyl peptidase II: the N-terminal part of the enzyme is similar to subtilisin. Biochemistry *30*, 168–174.

Udenfriend, S., Stein, S., Böhlen, P., Dairman, W., Leimgruber, W., and Weigele, M. (1972). Fluorescamine: a reagent for assay of amino acids, peptides, proteins, and primary amines in the picomole range. Science *178*, 871–872.

Walz, J., Tamura, T., Tamura, N., Grimm, R., Baumeister, W., and Koster, A. J. (1997). Tricorn protease exist as an icosahedral supermolecule in vivo. Mol. Cell *1*, 59–65.

Wang, J., Hartling, J.A., and Flanagan, J.M. (1997). The structure of ClpP at 2.3 Å resolution suggests a model for ATP-dependent proteolysis. Cell *91*, 447–456.

Wenzel, T., Eckerskom, C., Lottspeich, F., and Baumeister, W. (1994). Existence of a molecular ruler in proteasomes suggested by analysis of degradation products. FEBS Lett. *349*, 205–209.

Wolf, S., Nagy, I., Lupas, A., Pfeifer, G., Cejka, Z., Müller, S.A., Engel, A., De Mot, R., and Baumeister, W. (1998). Characterization of ARC, a divergent member of the AAA ATPase family from Rhodococcus erythropolis. J. Mol. Biol. *277*, 13–25.

Yen, C., Green, L., and Miller, C.G. (1980a). Degradation of intracellular protein in Salmonella typhimurium peptidase mutants. J. Mol. Biol. *143*, 21–33.

Yen, C., Green, L., and Miller, C.G. (1980b). Peptide accumulation during growth of peptidase deficient mutants. J. Mol. Biol. *143*, 35–48.

GenBank Accession Numbers

The accession numbers for the F2- and F3-encoding gene sequences reported in this paper are AF081951 and AF081952, respectively.